Ecohydrology of groundwater-dependent ecosystems: 1. Stochastic water table dynamics

Francesco Laio,[1] Stefania Tamea,[1,2] Luca Ridolfi,[1] Paolo D'Odorico,[3] and Ignacio Rodriguez-Iturbe[2]

Received 18 July 2008; revised 6 December 2008; accepted 19 December 2008; published 21 May 2009.

[1] Areas with a relatively shallow water table are environments where the groundwater plays a key role on the ecosystem function, and important interactions exist between hydrology and ecosystem processes. We propose here an analytical model to study the interactions between rainfall, water table, and vegetation in groundwater-dependent ecosystems. The water table dynamics are studied as a random process stochastically driven by a marked Poisson noise representing rainfall events. Infiltration, root water uptake, water flow to/from an external water body, and capillary rise are accounted for in a probabilistic description of water table fluctuations. We obtain analytical expressions for the steady state probability distribution of water table depth, which allows us to investigate the long-term behavior of water table dynamics, and their sensitivity to changes in climate, vegetation cover, and water management.

Citation: Laio, F., S. Tamea, L. Ridolfi, P. D'Odorico, and I. Rodriguez-Iturbe (2009), Ecohydrology of groundwater-dependent ecosystems: 1. Stochastic water table dynamics, *Water Resour. Res.*, *45*, W05419, doi:10.1029/2008WR007292.

1. Introduction

[2] Groundwater-dependent environments are areas where the groundwater plays a key role both on vegetation dynamics and on the soil water balance; possible examples include riparian zones, peatlands, and unsubmerged wetlands. These areas are of particular interest for several reasons, including their relatively high richness both in animal and plant species, and their ability to sequester and store carbon [*Mitsch and Gosselink*, 2000]. The dynamics of these ecosystems are controlled by the soil water balance and are affected by water table depth and soil water content. Water table fluctuations and soil moisture profiles, in fact, play a fundamental role in major ecohydrologic processes, including infiltration, surface runoff, groundwater flow, land-atmosphere feedbacks, vegetation dynamics, nutrient cycling, and pollutant transport. Understanding and modeling the soil water balance and its relationships with climate, soil and vegetation is therefore a crucial aspect for geosciences such as hydrology and ecology [*Rodriguez-Iturbe et al.*, 2007].

[3] Interactions between precipitation, soil water content and vegetation in water-controlled ecosystems have been studied in the recent past within the ecohydrology framework proposed by *Rodriguez-Iturbe et al.* [1999]. This process-based approach accounts for the random character of precipitation within simple models of soil moisture dynamics [see, e.g., *Laio et al.*, 2001; *Porporato et al.*, 2001; *Laio*, 2006]. These theoretical tools have been used to investigate the probabilistic dynamics of soil moisture, and applied to a variety of arid and semiarid ecosystems [e.g., *Rodriguez-Iturbe and Porporato*, 2004] characterized by scarce rainfall, relatively low average soil water content, recurrent water stress, and absence of a shallow water table. Since these soil water balance models did not account for the occurrence of long-lasting saturated conditions, their ecohydrological application has been so far limited to cases where the groundwater is so deep to exert no influence on the soil water balance.

[4] In the case of groundwater dependent ecosystems, the water table interacts with the root zone, supplying water to plants. The strong coupling between rainfall, vegetation, water table position and soil water content thus leads to important and interesting feedbacks between hydrological and ecosystem processes (see *Ridolfi et al.* [2006] and *Rodriguez-Iturbe et al.* [2007] for a detailed discussion).

[5] Water table and capillary rise play an active role in the subsurface water balance. Since the seminal work by *Eagleson* [1978], a remarkable amount of research has been carried out to investigate plant interaction with the stochastic dynamics of soil moisture. For example, *Salvucci and Entekhabi* [1994] studied numerically the fluxes and moisture states at different timescales and for different water table positions, and tested the reliability of an equivalent steady profile of soil moisture. The same authors [*Salvucci and Entekhabi*, 1995] investigated the coupled unsaturated-saturated flows throughout a hillslope; *Bierkens* [1998] studied the water table dynamics expressing environmental randomness through an additive Gaussian noise term; *Kim et al.* [1999] used a mixed analytical-numerical approach to investigate soil moisture patterns along an hillslope. However, although these studies have elucidated several important aspects of the interactions between soil water dynamics in the saturated and unsaturated zones, and their stochastic

[1]Dipartimento di Idraulica, Trasporti ed Infrastrutture Civili, Politecnico di Torino, Turin, Italy.
[2]Department of Civil and Environmental Engineering, Princeton University, Princeton, New Jersey, USA.
[3]Department of Environmental Sciences, University of Virginia, Charlottesville, Virginia, USA.

0043-1397/09/2008WR007292

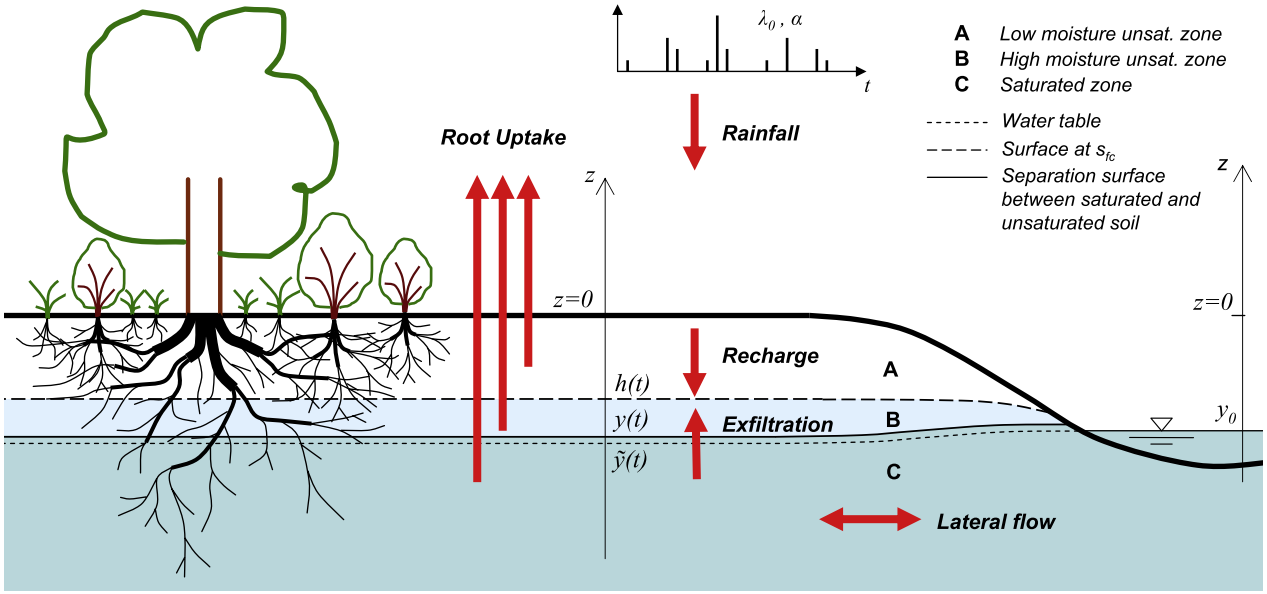

Figure 1. Scheme of the water fluxes in the soil column.

drivers, an analytical framework for the calculation of the probability distributions of soil moisture and water table depth is still missing. *Ridolfi et al.* [2008] have recently developed a probabilistic framework to investigate the coupled soil moisture–water table dynamics in the case of bare soil conditions (i.e., without vegetation), while a similar analytical model does not exist in the case of vegetated soils. To fill this gap, we propose a process-based probabilistic model of water table depth and soil moisture dynamics in the presence of plant roots interacting with saturated and unsaturated zones.

[6] The quantitative understanding of these complex dynamics requires a new process-based ecohydrological framework accounting for water table fluctuations, capillary rise, vertical distribution of soil moisture, and the complex mechanisms of plant water uptake. This framework is based on the soil water balance equation forced by stochastic precipitation. The water balance equation is explicitly solved at each infinitesimal horizontal soil layer by accounting for rainfall infiltration, water table recharge, plant water uptake, capillary rise, groundwater flow, and the coupling between water table fluctuations and soil moisture dynamics in the unsaturated portion of the soil column.

[7] In this paper we will consider the stochastic dynamics of the water table position, while we refer to the companion paper [*Tamea et al.*, 2009] for an explicit modeling of the soil moisture dynamics in groundwater-dependent ecosystems. Owing to the coupling between these two processes, some results presented in this paper are used and applied by *Tamea et al.* [2009], and vice versa.

2. Water Balance Equation

[8] We consider an infinitely deep soil column and use an upward oriented vertical axis, z, with $z = 0$ at the ground surface (see Figure 1). Soil properties such as effective porosity, n, grain size distribution, and water retention curves, are assumed to be uniform in space and constant in time. The horizontal area of interest is the plot scale (e.g., $1-100\ m^2$) and is supposed to be reasonably flat. We will not consider local heterogeneities in soil and vegetation, nor topographic gradients or regional groundwater dynamics. The water content existing at any point of the soil column is expressed in terms of soil moisture, s ($0 \le s \le 1$). The soil matric potential, ψ (negative), and unsaturated hydraulic conductivity, k, are related to soil moisture s through the *Brooks and Corey* [1964] model, truncated at small values of hydraulic conductivity,

$$\psi(s) = \psi_s s^{-1/m}; \quad k(s) = \begin{cases} k_s s^{(2+3m)/m} & \text{if } s_{fc} < s \le 1, \\ 0 & \text{if } s \le s_{fc}, \end{cases} \tag{1}$$

where ψ_s is the (negative) air entry pressure head or saturated soil matric potential, m is the pore size index, s_{fc} is the soil moisture at field capacity, and k_s is the saturated hydraulic conductivity. Field capacity is the water content held in the soil after gravity drainage [e.g., *Hillel*, 1998]; s_{fc} is operationally defined as the soil water content at which the unsaturated hydraulic conductivity becomes negligible if compared to other fluxes into the soil [see also *Laio et al.*, 2001; *Laio*, 2006]. In particular, we take as a reference flux the potential evapotranspiration rate, T_p, and define s_{fc} from the relation $k(s_{fc}) = 0.05\ T_p$, finding

$$s_{fc} = \left(\frac{0.05 T_p}{k_s}\right)^{\frac{m}{2+3m}}. \tag{2}$$

The values obtained with this relationship are coherent with those obtained with more classical definitions, such as the moisture corresponding to a soil matric potential of -0.33 MPa (see Table 1 in the work of *Tamea et al.* [2009]).

[9] Typically, three zones can be identified in the soil column, according to the local water content. Starting from the bottom, one finds (see Figure 1): (1) the saturated zone, where all the soil pores are filled with water (i.e., $s = 1$); (2) the unsaturated zone with high soil moisture (HM), where the water content is larger than field capacity (i.e., $s_{fc} \le s < 1$);

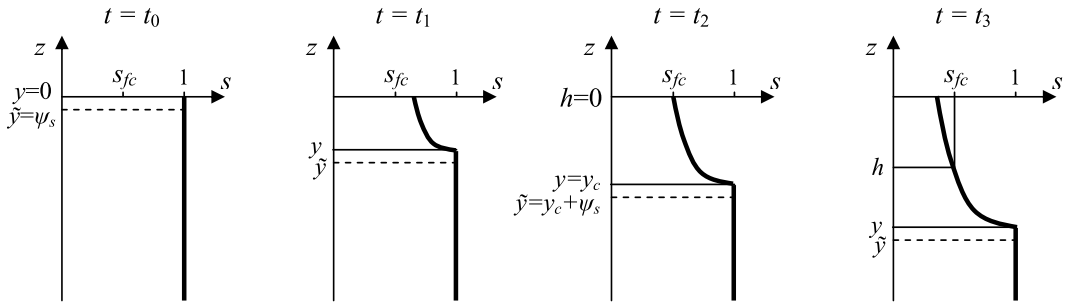

Figure 2. Sketch of the water table position and soil moisture dynamics in a soil drying phase.

and (3) the unsaturated zone with low soil moisture (LM), where the water content is smaller than field capacity (i.e., $s < s_{fc}$). The high moisture zone is characterized by large values of the hydraulic conductivity, while in the low moisture zone, the hydraulic conductivity is assumed to be negligible, as in equation (1). The boundary between these zones is the layer at field capacity, found at a depth $h(t)$ from the soil surface (where t is time).

[10] The water table, defined as the saturated soil surface at zero pressure, lays at depth $\tilde{y}(t)$ from the soil surface, variable in time t. The soil above the water table is saturated up to a constant distance $|\psi_s|$ from $\tilde{y}(t)$, where the soil matric potential equals the (negative valued) ψ_s. As a consequence, the separation between saturated and unsaturated soil occurs at a depth

$$y(t) = \tilde{y}(t) - \psi_s, \tag{3}$$

and this separation surface is of particular interest for our modeling scheme (see Figure 1). In fact, it will be convenient to model the dynamics of the water table by means of the variable $y(t)$, i.e., the separation surface between saturated and unsaturated soil. The results corresponding to the water table position, $\tilde{y}(t)$, can then be obtained with the simple relation (3), which rigidly links the dynamics of $y(t)$ and $\tilde{y}$.

[11] In order to quantitatively study the water table dynamics, one needs to establish a water balance equation relating the variations in time of the water table position to the incoming and outgoing fluxes. The balance equation reads:

$$\begin{aligned}(\textit{Specific yield}) \cdot \frac{\mathrm{d}\tilde{y}(t)}{\mathrm{d}t} &= (\textit{Specific yield}) \cdot \frac{\mathrm{d}y(t)}{\mathrm{d}t} \\ &= \textit{Recharge} \pm \textit{Lateral flow} - \textit{Uptake} \\ &\quad - \textit{Exfiltration}. \end{aligned} \tag{4}$$

The variations in time of the water table position, and correspondingly of $y(t)$, are modulated by the specific yield, which is the ratio between the volume of water released from storage (per unit cross-sectional area of the aquifer) and the corresponding drop in water table elevation. Four fluxes play a role in the y dynamics (see Figure 1): recharge, i.e., the infiltration rate that reaches the saturated zone; lateral flow to or from an external water body; root uptake from the saturated zone; exfiltration from the saturated zone due to capillary rise. In equation (4) and in the rest of the paper we neglect the effect of evaporation, which is small compared to transpiration when a dense vegetation cover is present.

[12] To better understand the role played by the terms in equation (4) in the dynamics of $y(t)$, and the factors contributing to the partitioning of the soil column into the saturated and unsaturated (HM and LM) zones, we consider as an example the case of a soil column that reaches complete saturation (i.e., $y = 0$) in the course of a rainfall event (as shown in Figure 2). At a certain time, $t = t_0$, when $y(t_0) = 0$, the rain stops and the soil starts drying out. At this point the recharge rate tends to zero while root uptake, lateral flow, and exfiltration induce a water loss from the soil column; the upper soil layers start drying out, y decreases, and a nonuniform profile of soil moisture establishes. The shape of this profile is dictated by the balance between the capillary flux from the saturated zone, and root uptake from the high moisture zone, as detailed in section 3.4. At time $t = t_1$ soil moisture is still larger than s_{fc} in all layers. Thus, at this time there is no low moisture zone. At a time t_2 soil moisture is at field capacity at the ground surface (i.e., $s(0) = s_{fc}$) and $h(t_2) = 0$. The critical depth, y_c, at which $h(t) = 0$ marks the transition between two regimes: a shallow water table (SWT) regime for $y > y_c$, and a deep water table (DWT) regime for $y \leq y_c$. The properties of these two regimes will be discussed in detail in the following sections. If soil drying continues for $t > t_2$ the soil water content in the upper portion of the soil column attains soil moisture values below field capacity (see Figure 2) and y is deeper than y_c. As a consequence, it is only when $y > y_c$, i.e., only under DWT conditions, that a low moisture zone is present in the soil column. In the following two sections we express the terms of the water balance equation (4), under shallow (section 3) and deep (section 4) water table conditions.

3. Model Specification Under Shallow Water Table Conditions

[13] The following representation of the water balance equation (4) is valid under shallow water table conditions:

$$\beta(y)\frac{\mathrm{d}y(t)}{\mathrm{d}t} = Re(t) + f_l(y) - U_s(y) - Ex(y), \tag{5}$$

where $\beta(y)$ is the specific yield, which depends on the water table position, and then on the depth y; $Re(t)$ is the recharge rate; $f_l(y)$ is the lateral flow to or from an external water body; $U_s(y)$ is the plant water uptake from the saturated zone; $Ex(y)$ is the exfiltration flux due to capillary rise. The single components of this balance equation are described in the following sections.

3.1. Recharge Rates

[14] Groundwater recharge is the result of rainfall infiltration and redistribution through the soil column. Suitable representations of these processes (precipitation, infiltration and redistribution) are therefore required. Rainfall is the main input of water into the soil column. Following previous studies [e.g., *Rodriguez-Iturbe et al.*, 1999; *Laio et al.*, 2001], rainfall is here taken as a stochastic forcing and represented, at the daily timescale, as a marked Poisson process, $\mathcal{P}(\lambda, \alpha)$, with rate λ and exponentially distributed rainfall depths with mean α. Precipitation lost before infiltration includes canopy interception, which acts on rainfall as a threshold filter preserving the Poissonian nature of the forcing but reducing the frequency of the wetting events. The net rate is thus $\lambda_0 = \lambda e^{-\delta/\alpha}$, where δ is the threshold for canopy interception [*Rodriguez-Iturbe et al.*, 1999].

[15] The processes of infiltration and redistribution in the high moisture zone are modeled as a soil moisture wave propagating downward as a piston flow [see *Laio*, 2006; *Botter et al.*, 2007] and are considered to occur instantaneously (at the daily timescale). In fact, because in SWT conditions soil moisture values are larger than s_{fc} in all soil layers, the unsaturated hydraulic conductivity (from equation (1)) of most soils is large enough to assume that (at the daily timescale) water redistribution within the high moisture zone occurs instantaneously, thereby contributing to groundwater recharge. In fine-grained soil with a smaller hydraulic conductivity, the instantaneous redistribution is enabled by a field capacity close to saturation, which leads to small moisture gradients and quick redistribution within the high moisture zone. In these conditions groundwater recharge occurs as a sequence of events that matches that of rainfall occurrences; as such, it can be modeled as a Poisson process with rate λ_0 and exponential probability distribution of the recharge depths (with mean α),

$$Re(t) = \mathcal{P}(\lambda_0, \alpha). \tag{6}$$

The recharge depths are then converted into variations of the water table position through the specific yield, $\beta(y)$ (see section 3.5).

3.2. Lateral Flow

[16] The presence of a nearby water body can be associated with a lateral flow, which may have an important effect on the water table dynamics. In fact, inflow or outflow takes place, depending on the relative position of the water surface (in the water body) and of the water table at the site under investigation. The form of the term $f_l(y)$ in the water balance equation (5) depends on the geometry of the system.

[17] We will consider the case of a water body at a level y_0 constant in time and at a distance large enough to allow for the water table to be subhorizontal at the site under consideration (see Figure 1). Under these conditions the lateral flow can be approximately expressed through the Darcy's law,

$$f_l(y) = k_l(y_0 - \tilde{y}) = k_l(y_0 - y - \psi_s), \tag{7}$$

i.e., as a linear function of the difference between y_0 and the water table depth, $\tilde{y}$, with a constant of proportionality, k_l.

3.3. Root Uptake From the Saturated Zone

[18] A key aspect in the evaluation of groundwater-vegetation interactions is the mechanism of plant water uptake. Root functioning plays a central role on the ecohydrological dynamics of humid land ecosystems, and on the complex feedbacks between abiotic and biotic factors. On the one hand, water table dynamics affect the vertical distribution of roots, as the frequency and duration of flooding are determinant for root growth strategies [*Naumburg et al.*, 2005] and plant resources allocation [e.g., *Ho et al.*, 2004]. On the other hand, root uptake decreases the soil water content and contributes to lower the water table position. A significant local drop occurs, for example, during the day due to the relevant water uptake driven by photosynthetic and physiological demand. A partial recovery occurs at night due to groundwater redistribution, thereby inducing regular day-night water table fluctuations [see, e.g., *Loheide et al.*, 2005]. Nevertheless, because the present analysis is carried out at the daily timescale, oscillations occurring at subdaily timescales are not resolved. Thus, in the absence of rainfall only the transpiration-induced decreasing trends in soil water content and water table elevation are considered.

[19] In general, prolonged flooded conditions lead to plant water stress and anoxia and can ultimately result in the death of submerged roots. However, plant species populating humid lands and wetlands may be well adapted to soil anoxic conditions and could cope with soil saturation adopting different strategies to survive waterlogging. For example they may have anaerobic metabolisms and may be able to increase oxygen provision to the roots [e.g., *Naumburg et al.*, 2005; *Vartapetian and Jackson*, 1997]. Strategies of water uptake and ability to work in anoxic conditions are peculiar of each plant species [*Naumburg et al.*, 2005]. For example, the nonspecialized mesophytes take up water mostly from the shallower soil and undergo water stress conditions if rainfall is highly intermittent. Phreatophytes, on the other hand, typically consume groundwater and are more resistent to drought stress [*Meinzer*, 1927; *Robinson*, 1958]. As an extreme case, hydrophytes live in submerged wetlands and have roots constantly flooded.

[20] At the field scale there is coexistence of species with different root allocation strategies; however, we are interested in the overall, plot-scale, behavior of the groundwater-dependent ecosystem. As a consequence, we make some simplifying assumptions on the functioning of root uptake:

[21] 1. The uptake flux is unaffected by anoxic (saturated) conditions in the soil; i.e., no uptake-reduction function is applied for large s values.

[22] 2. A noncooperative root functioning is considered, which neglects compensation mechanisms [see, e.g., *Guswa*, 2005, 2008]: roots in each soil layer take up water independently of the others and do not compensate for limitations in transpiration and uptake, which may occur somewhere along the soil profile.

[23] 3. A simple function $r(z)$ is adopted to represent the plot-scale averaged root distribution. Following other authors [e.g., *Schenk and Jackson*, 2002; *Schenk*, 2005; *Laio*, 2006], we consider an exponential distribution of the root biomass, $r(z) = 1/b \cdot e^{z/b}$ where b is the average rooting depth.

[24] Under these assumptions, plant water uptake from a soil layer at a depth, z, in the saturated or unsaturated high moisture zone equals $T_p \cdot r(z)$, where T_p is the maximum potential evapotranspiration, which is controlled by atmospheric conditions, such as net solar irradiance, wind speed, air temperature, and humidity. As a consequence, the total root uptake from the saturated zone is

$$U_s(y) = T_p \int_{-\infty}^{y} r(z)\mathrm{d}z = T_p e^{y/b}. \tag{8}$$

3.4. Exfiltration Rate

[25] Exfiltration is the upward vertical movement of water (capillary rise) from saturated to partially saturated soil layers. *Ridolfi et al.* [2008] studied capillary rise and exfiltration in bare soil conditions, i.e., in the absence of root uptake. In that particular case, the capillary flux is driven by differences in soil matric potential induced by bare soil evaporation. In the presence of root uptake the situation is different: the capillary flux is still driven by differences in soil matric potential in the soil layers, but now these differences are induced by uptake rather than evaporation. This changes the mechanics of the capillary flux, in that plant roots take up water at different depths in the soil, depending on where roots are allocated, while evaporation acts only at the soil surface. Thus, under bare soil conditions, all water exfiltrating from the saturated zone reaches the soil surface, and the capillary flux is constant at all depths, z.

[26] In contrast, when vegetation is present (and evaporation is negligible) the capillary flux, $v(z)$, varies with z, due to water withdrawal by roots. To understand and model the functional dependence of v on z, we consider the water balance equation for a horizontal infinitesimal soil layer at a depth z, in the high moisture unsaturated zone (the "z layer"). The balance equation is

$$n\frac{\partial s_y(z,t)}{\partial t} = \frac{\partial v(z,t)}{\partial z} - T_p r(z) \tag{9}$$

where n is the soil porosity, $s_y(z, t)$ is the (y-dependent) soil water content in the z layer at time t, and $\frac{\partial v(z,t)}{\partial z}$ represents the difference between the capillary flux entering the layer at a depth z and exiting at the depth $z + \mathrm{d}z$, at time t.

[27] We suppose that $s_y(z, t)$ varies slowly in time (at the daily timescale), responding to variations in y; thus we represent the dynamics of $s_y(z)$ and $v(z)$ as a sequence of stationary states, obtaining from equation (9)

$$\frac{\mathrm{d}v(z)}{\mathrm{d}z} = T_p r(z) = \frac{T_p}{b} e^{z/b}. \tag{10}$$

Integration between 0 and z, with boundary condition $v(0) = 0$ due to the assumption of negligible evaporation, provides $v(z) = T_p(1 - e^{z/b})$. Since the exfiltration flux leaving the saturated zone, $Ex(y)$, is the capillary flux at depth y, i.e., $v(y)$, one finally obtains

$$Ex(y) = T_p\left(1 - e^{y/b}\right). \tag{11}$$

If this result is combined with equation (8) one finds that, under shallow water table conditions, the total flux from the saturated zone (leaving aside the lateral flow) is constant and equal to the potential evapotranspiration rate, $U_s(y) + Ex(y) = T_p$.

3.5. Specific Yield

[28] The specific yield is the ratio between the volume of water, V_w, an aquifer releases or takes into storage, per unit aquifer area, and the corresponding change in water table depth, Δ [*Freeze and Cherry*, 1979]. It is in general dependent on soil properties and water table depth. More specifically, when modeling the water table dynamics, we are interested in the limit of the specific yield for infinitesimal variations of the water table depth,

$$\beta(y) = \lim_{\Delta \to 0} \frac{V_w}{\Delta}. \tag{12}$$

In the evaluation of the specific yield, we do not account for the continuous time dependence in the dynamics of the soil moisture profile [e.g., *Nachabe*, 2002; *Hilberts et al.*, 2007], rather we assume that the profile evolves, at the daily scale, as a succession of instantaneous steady states. Several expressions for the specific yield have been formulated [e.g., *Duke*, 1972; *Nachabe*, 2002], but none of them is fully consistent with our modeling framework. We therefore evaluate $\beta(y)$ based on its definition (equation (12)).

[29] The volume V_w, e.g., released by an increase of water table depth, can be determined from the soil moisture profiles using the relation

$$V_w = n\left[\int_{s_{y+\Delta}(0)}^{1} z_{y+\Delta}(s)\mathrm{d}s - \int_{s_y(0)}^{1} z_y(s)\mathrm{d}s\right], \tag{13}$$

where $s_y(0)$ is the soil moisture content at the soil surface when the separation surface between saturated and unsaturated soil lays at depth y, and $z_y(s)$ is the soil moisture profile, expressed using the soil moisture content s as the independent variable, and z as the dependent variable. A Taylor expansion of $z_{y+\Delta}(s)$ around $\Delta = 0$, truncated to the first order, provides $z_{y+\Delta}(s) = z_y(s) + \frac{\partial z_y(s)}{\partial y}\Delta$, which can be set in equation (13) to give

$$V_w = n\left[\int_{s_y+\Delta(0)}^{1} \frac{\partial z_y(s)}{\partial y}\Delta\mathrm{d}s - \int_{s_y(0)}^{s_y+\Delta(0)} z_y(s)\mathrm{d}s\right]. \tag{14}$$

For $\Delta \to 0$ the second addendum tends to $[s_{y+\Delta}(0) - s_y(0)]z_y(s_y(0))$, which in turn tends to zero because $z_y(s_y(0)) = 0$. The specific yield can be then expressed as

$$\beta(y) = \lim_{\Delta \to 0} \frac{V_w}{\Delta} = n\int_{s_y(0)}^{1} \frac{\partial z_y(s)}{\partial y}\mathrm{d}s. \tag{15}$$

[30] A suitable approximation of the soil moisture profile needs to be specified in order to obtain an expression for the specific yield. The relation between soil moisture, s (or soil matric potential ψ) at depth, z, below the soil surface, and the depth, y, of the separation surface between saturated and unsaturated soil can be obtained using a steady state

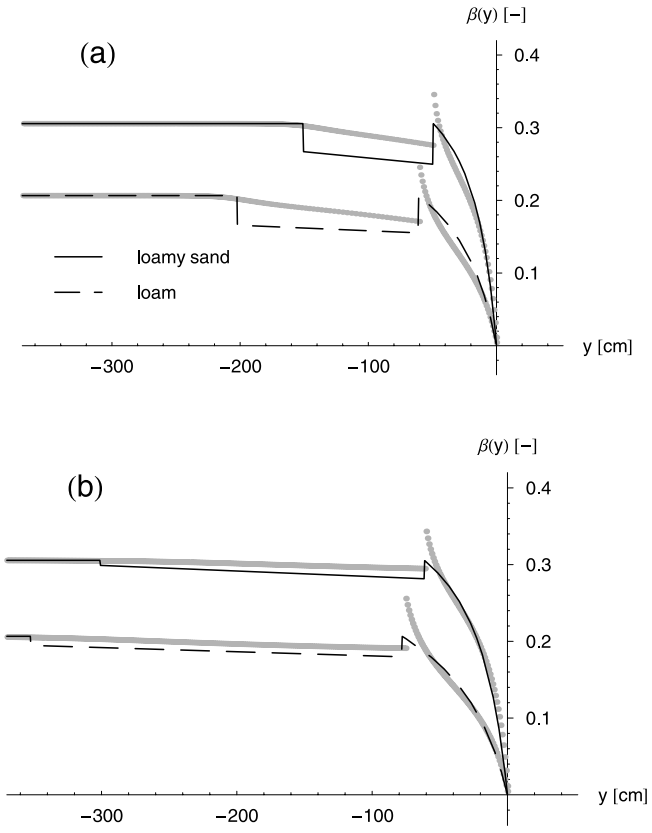

Figure 3. Specific yield, β, as a function of the separation depth, y, in a loamy sand and a loam, for two mean root depths: (a) b = 10 cm and (b) b = 40 cm. Comparison between the numerical results (gray dots) and the approximations presented in the paper (continuous and dashed lines).

approximation of Richard's equation, with an additional sink term $T_p \cdot r(z)$ due to root uptake:

$$\frac{\partial}{\partial z}\left[k(\psi)\left(\frac{\partial \psi}{\partial z}+1\right)\right] = T_p r(z). \tag{16}$$

Using the relations in equation (1) and the exponential form of the root profile, one obtains after integration between z and 0

$$-k_s s^{(2+3m)/m}\left(1-\frac{\mathrm{d}s}{\mathrm{d}z}\frac{\psi_s}{m}s^{-(1+m)/m}\right) = T_p\left(1-e^{z/b}\right) \tag{17}$$

where the last term is the steady state, z-dependent, capillary flux, $v(z)$ (see section 3.4) and $s = s_y(z)$, i.e., the depth-dependent soil moisture in the HM unsaturated zone.

[31] Equation (17) cannot be solved analytically. We therefore approximate the relation between s, z and y through the expression

$$s_y(z) = \left[1+\left(s_{fc}^{-1/(2m)}-1\right)\left(\frac{y-z}{y_c}\right)\right]^{-2m} \tag{18}$$

where y_c is the critical value of the depth y, marking the passage between shallow and deep water table conditions (see section 3.6). The suitability of this expression to represent the actual soil moisture profile is investigated in the companion paper [*Tamea et al.*, 2009]. The inversion of equation (18) yields

$$z_y(s) = y - y_c\left(\frac{s^{-1/(2m)}-1}{s_{fc}^{-1/(2m)}-1}\right). \tag{19}$$

From equation (18) we have that $\frac{\partial z_y(s)}{\partial y} = 1$. Thus, using equation (15) the specific yield can be expressed as

$$\beta(y) = n\left[1-s_y(0)\right] = n - n\left[1+\left(s_{fc}^{-1/(2m)}-1\right)\left(\frac{y}{y_c}\right)\right]^{-2m}. \tag{20}$$

[32] A representation of the specific yield as a function of the depth y is reported in Figure 3. The part of Figure 3 corresponding to equation (20) is at the right of the critical depth, where $y > y_c$. The specific yield approaches zero for $y \to 0$ because of the small storage capacity (and high soil water content) in the unsaturated zone when y approaches the soil surface.

3.6. Critical Depth y_c

[33] In our schematic representation of the soil column, the critical value of y, i.e., y_c, marks the transition between shallow and deep water table conditions, defined in section 2. To determine the exact value of y_c one should integrate equation (17) and impose the boundary condition $s(0) = s_{fc}$. However, no analytical solutions can be found. A valid approximation is obtained using in equation (17) a suitable z-independent rate of capillary flux, $v^* = \frac{T_p}{1+c_0 b} = \frac{T_p}{1+(0.35-0.65n)b}$ (see Figure 4). The solution of equation (17) with $v(z) = v^*$ [*Ridolfi et al.*, 2008] leads to

$$y_c = \psi_s s_{fc}^{-1/m} F_1\left[\frac{1}{2+3m}, 1, 1+\frac{1}{2+3m}, -\frac{v^*}{k_s}s_{fc}^{-(2+3m)/m}\right] - \psi_s F_1\left[\frac{1}{2+3m}, 1, 1+\frac{1}{2+3m}, -\frac{v^*}{k_s}\right], \tag{21}$$

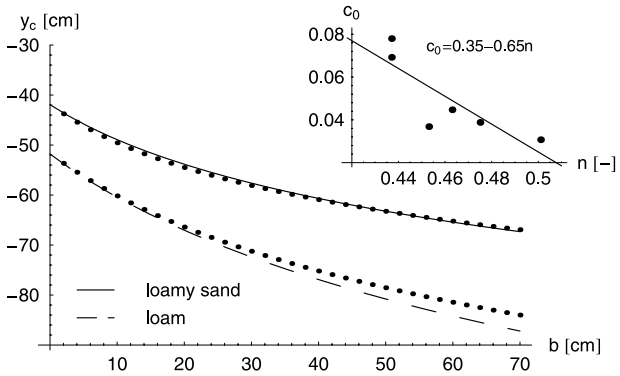

Figure 4. Influence of the mean root depth, b, on the critical depth, y_c, for a loamy sand and a loam. The dots correspond to the numerical solution, while the lines represent the approximation of y_c given by equation (21). The functional dependence of v^* on b is found to be of the form $T_p/v^* = 1 + c_0\, b$, where the parameter c_0 is correlated to the soil porosity n (see inset).

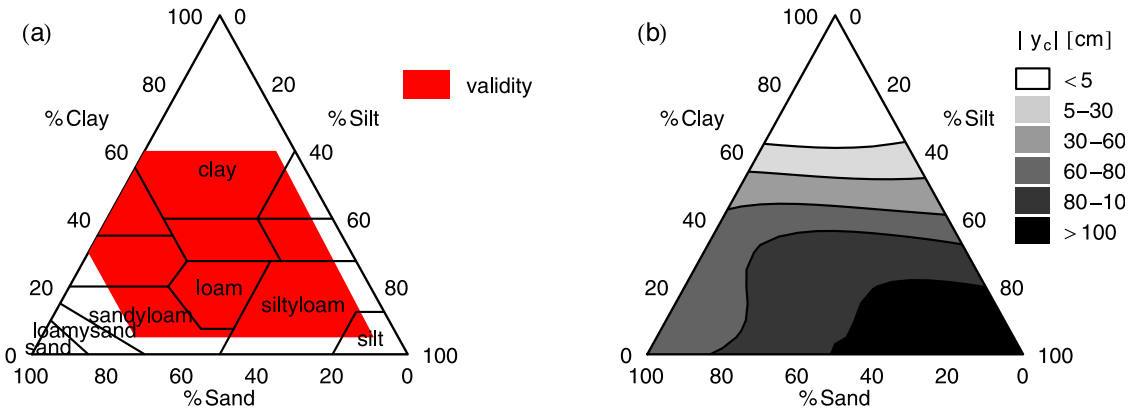

Figure 5. USDA soil texture triangle: (a) validity zone for the empirical pedotransfer functions relating soil hydraulic parameters and soil composition [see *Rawls and Brakensiek*, 1989], and (b) the critical depth, y_c, computed across different soils, for a mean root depth b of 30 cm.

where $F_1[a, b, c, x]$ is the hypergeometric function [*Abramowitz and Stegun*, 1965].

[34] The validity of the approximate solution (equation (21)) is shown in Figure 4 in a comparison with the numerical solution of equation (17), for different soil types and different values of the average rooting depth b. Figure 4 clearly shows that equation (21) provides a good approximation of the critical depth.

[35] Figure 5b shows the variability of the critical depth y_c across different soils, represented in the USDA soil texture triangle [*Soil Conservation Service*, 1975]. y_c is of the order of some tens of centimeters, and tends to be larger in silty soils compared to sandy and clayish soils. A deeper rooting system causes a decrease of the capillary flux in the upper soil layers, thereby inducing a slight deepening of y_c (not shown). Notice that in clayey soils, the pedotransfer functions between soil composition and hydraulic parameters are not valid [see *Rawls and Brakensiek*, 1989, p. 279] (see also Figure 5a). Since these relationships have been used to draw Figure 5b, the top part of the USGS triangle shows results of uncertain reliability, due to the extrapolation of hydraulic parameter values.

4. Model Specification Under Deep Water Table Conditions

[36] The following representation of the water balance equation (4) is valid under deep water table (DWT) conditions, i.e., for $y < y_c$:

$$\beta(h,y)\frac{\mathrm{d}y(t)}{\mathrm{d}t} = Re\left(h,\overline{s}'_m(h),t\right) + f_l(y) - U_s(y) - Ex(h,y). \quad (22)$$

The lateral flux and uptake terms are the same as in SWT conditions (equations (7) and (8)). The rates of recharge $Re(h, \overline{s}'_m(h), t)$, and exfiltration, $Ex(h, y)$, and the specific yield, $\beta(h, y)$, in contrast, need to be expressed differently, as explained in the following sections.

4.1. Recharge Rate

[37] The recharge rate is linked to the rainfall rate as in the case of the shallow water table. However, in the case of deep water table not all rain events are actually able to reach the high moisture zone. Each rain event generates a wetting front which separates soil layers whose water content, s, is supposed to instantaneously (at the daily timescale) reach field capacity from layers which remain unaffected. The hypothesis of instantaneous redistribution in the low moisture zone is supported by the numerical simulations carried out by *Laio* [2006, section 2.1]. The depth reached by the wetting front depends on the rain depth and on the soil moisture content before the event. Only some of the events recharge the groundwater, $Re(h, \overline{s}'_m(h), t)$. These are the events generating a wetting front that reaches the top of the high moisture zone, where, since $s \geq s_{fc}$, water is instantaneously drained toward deeper layers. The instantaneous redistribution in the high moisture zone is enabled in coarse-grained soils by the large values of hydraulic conductivity, and in fine-grained soils by a field capacity close to saturation, which leads to small moisture gradients within the high moisture zone. The sequence of these recharge events is stochastic due to the random nature of rainfall. In general this sequence is non-Poissonian; however, *Laio* [2006] showed that the recharge process retains the Poissonian properties of rainfall occurrences if one assumes that all rainfall events find the same average soil moisture content, $\overline{s}'_m(h)$, in the low moisture zone. Under this assumption, the recharge rate will not depend on the fluctuations of $s(z)$ but only on the local long-term average values.

[38] Note that $\overline{s}'_m(h) = -\frac{1}{h}\int_h^0 \overline{s}'(z)\,\mathrm{d}z$, where $\overline{s}'(z)$ is the long-term average of the soil moisture content in the layer at a depth z, conditional upon $s < s_{fc}$ (because the occurrence of recharge events depends only on the soil water content above $z = h$). In this case the water storage capacity in the soil column above h is $-nh[s_{fc}-\overline{s}'_m(h)]$; i.e., it depends on h but not on $s(z)$. As a consequence, the sequence of recharge events remains Poissonian [*Laio*, 2006]; its rate can be determined as in the case of canopy interception (see section 3.1 and *Laio* [2006]),

$$\lambda\left[h,\overline{s}'_m(h)\right] = \lambda_0 \exp\left[\frac{nh\left(s_{fc}-\overline{s}'_m(h)\right)}{\alpha}\right], \quad (23)$$

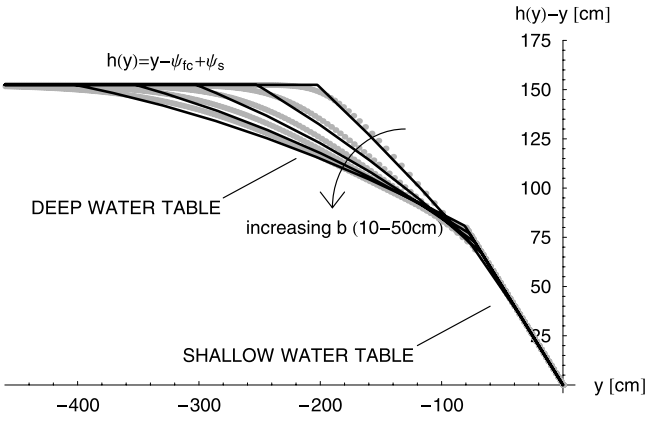

Figure 6. Height of the high moisture unsaturated zone, $(h-y)$, as a function of the position of the separation surface, y, in a loamy soil and for various mean root depths (i.e., b = 10, 20, 30, 40 and 50 cm). Gray dots represents the numerical solution of the Richard's equation for the HM zone, while the continuous line is the piecewise approximation given in equation (26). Notice that below the bulk of the root zone, i.e., depth $(\psi_{fc}-\psi_s-5b)$, the distance between h and y becomes constant.

and the recharge depths are exponentially distributed with mean α. Using the same notation as in equation (6), one then has

$$Re\left(h,\overline{s}'_m(h),t\right)=\mathcal{P}\left(\lambda\left[h,\overline{s}'_m(h)\right],\alpha\right). \tag{24}$$

[39] The water table dynamics (equation (22)) under DWT conditions depend on the soil water content in the low moisture zone through the long-term average soil moisture $\overline{s}'_m(h)$. Because of this dependence, the water table dynamics are intertwined to those of soil moisture in the overlying layers. The vertical profile of average soil moisture in the low moisture zone is in turn related to the local climate (precipitation and potential evapotranspiration) and to the vertical distribution of roots [e.g., *Laio et al.*, 2006]. In the companion paper [*Tamea et al.*, 2009], we investigate in detail the soil moisture dynamics and provide a suitable representation of $\overline{s}'_m(h)$ for the case when plant roots are exponentially distributed with root density function $r(z)$.

[40] Note that, while $s'(z)$ affects y through the recharge rate, y does not affect the dynamics of soil moisture in the low moisture zone. In fact, we assume that the capillary flux through the surface at $z = h$ is negligible compared to the other fluxes occurring where $s \le s_{fc}$, and the depth h will be referred to as zero-flux surface. As a consequence of the absence of upward flux through the surface at a depth h, the low moisture zone can be considered as a stand-alone system, not related to the high moisture zone below it. Thus, soil moisture dynamics in the LM zone (i.e., the dynamics of $s'(z)$) can be studied as in the case of water-limited ecosystems [e.g., *Laio et al.*, 2001; *Laio*, 2006], without considering the presence of the water table. The overall dynamics of $s(z)$ will then result from the combination of periods when $s(z) = s'(z)$ (when $z > h$) and periods when the dynamics of $s(z)$ are deterministically related to those of y (when $z < h$), i.e., $s(z) = s_y(z)$ [see *Tamea et al.*, 2009].

4.2. Exfiltration Rate

[41] Exfiltration in DWT conditions is modeled similarly to the case presented in section 3.4: we consider the water balance equation for an infinitesimal soil layer in the high moisture unsaturated zone. As noted, if we model the dynamics of $s_y(z)$ as a sequence of steady states, we obtain equation (10), which integrated from h to z gives the capillary flux at the generic depth z in the HM zone, $v(z) = T_p\ (e^{h/b} - e^{z/b})$. The boundary condition $v(h) = 0$ is imposed, which descends from the assumption of null hydraulic conductivity for $s < s_{fc}$ (see equation (1)), i.e., above h. The overall exfiltration flux out of the saturated zone is then

$$Ex(h,y)=v(y)=T_p\left(e^{h/b}-e^{y/b}\right). \tag{25}$$

stating that exfiltration from the saturated zone is balanced by root uptake in the high moisture unsaturated zone. Owing to the absence of capillary flux in the low moisture zone, the depth h represents the threshold above which the water table exerts no influence on the local soil water balance.

[42] To complete the representation of the exfiltration process it is still necessary to establish the relation between the depths y and h, lower and upper boundary of the high moisture unsaturated zone, respectively. The soil moisture profile in the HM zone, $s_y(z)$, is obtained integrating equation (17), with $v(z) = T_p(e^{h/b} - e^{z/b})$ and boundary condition $s_y(h) = s_{fc}$. The corresponding depth of the separation surface between saturated and unsaturated zones is then determined by setting $s_y(y) = 1$. However, this procedure does not lend itself to analytical solutions. Accurate results are obtained when $h(y)$ is approximated by the stepwise function

$$h(y)=\begin{cases}0 & \text{if } y\ge y_c,\\ \left(1-A^{3/4}\right)(y-y_c)-\dfrac{A^2\left(1-A^{-1/4}\right)}{-y_c+\psi_{fc}-\psi_s}(y-y_c)^2 & \text{if } -5b+\psi_{fc}-\psi_s\le y<y_c,\\ y-\psi_{fc}+\psi_s & \text{if } y<-5b+\psi_{fc}-\psi_s,\end{cases} \tag{26}$$

where $A=\frac{\psi_{fc}-\psi_s-y_c}{\psi_{fc}-\psi_s-y_c-5b}$ and $\psi_{fc}=\psi_s s_{fc}^{-1/m}$. Note that the distance between h and y remains constant (and equal to $\psi_s - \psi_{fc}$) when the root density declines to zero, i.e., when h is much deeper than the average rooting depth, b (see Figure 6). The value of $(h-y)$ is then constant as a

consequence of the fact that at such depth the soil moisture profile approaches the zero-flux profile. The robustness of this approximation (26) has been extensively tested for different soils and values of b through a comparison with the numerical solution. An example of these comparisons is shown in Figure 6.

4.3. Specific Yield

[43] We follow an approach analogous to the one used for the case of shallow water table (section 3.5) and define the specific yield under DWT conditions as

$$\beta(y,h) = \frac{n}{\Delta}\int_{s_{fc}}^{1}\left[z_{y+\Delta}(s) - z_y(s)\right]\mathrm{d}s = n\int_{s_{fc}}^{1}\frac{\partial z_y(s)}{\partial y}\mathrm{d}s, \quad (27)$$

where the term on the right hand side results from the Taylor's expansion of $z_{y+\Delta}(s)$ around Δ truncated to the first order. The specific yield depends on h through the soil moisture profile $z_y(s)$, whose shape, in turn, depends on h. In fact, we can represent the soil moisture profile in the high moisture zone with an equation similar to (18), i.e.,

$$s_y(z) = \left[1 + \left(s_{fc}^{-1/(2m)} - 1\right)\left(\frac{y-z}{y-h}\right)\right]^{-2m}. \quad (28)$$

[44] The suitability of this expression to represent the actual soil moisture profile is investigated in detail by *Tamea et al.* [2009]. The inversion of equation (28) leads to

$$z_y(s) = y - (y-h)\left(\frac{s^{-1/(2m)} - 1}{s_{fc}^{-1/(2m)} - 1}\right), \quad (29)$$

which implies $\frac{\partial z_y(s)}{\partial y} = 1 - (1 - \frac{\mathrm{d}h}{\mathrm{d}y})\,(\frac{s^{-1/(2m)}-1}{s_{fc}^{-1/(2m)}-1})$. By setting this value in equation (27) one obtains

$$\begin{aligned}\beta(y,h) &= n\left(1 - s_{fc}\right) + n\left(\frac{\mathrm{d}h}{\mathrm{d}y} - 1\right)\int_{s_{fc}}^{1}\frac{s^{-1/(2m)} - 1}{s_{fc}^{-1/(2m)} - 1}\mathrm{d}s \\ &= n\left(1 - s_{fc}\right) + n\left(\frac{\mathrm{d}h}{\mathrm{d}y} - 1\right)B, \end{aligned} \quad (30)$$

with coefficient $B = \frac{1}{1-2m}\,(\frac{1-s_{fc}}{1-s_{fc}^{1/(2m)}} + 2ms_{fc})$. Figure 3 shows the results obtained with equation (30) and compares them with numerical simulations of the Richard's equation. When the water table is relatively deep ($y < -5b - \psi_s + \psi_{fc}$), the specific yield attains a constant value, $\beta(y, h) = n(1 - s_{fc})$, because $\frac{\mathrm{d}h}{\mathrm{d}y} = 1$. For $-5b - \psi_s + \psi_{fc} < y < y_c$, $\beta(y, h)$ tends to slightly decrease as $y \to y_c$, with a jump at $y = -5b - \psi_s + \psi_{fc}$ due to the approximation of $h(y)$ with a function with discontinuous derivative (equation (26)). At the critical depth $y = y_c$, the specific yield has another discontinuity due to the abrupt change in the derivative of $Ex(y)$ (see equations (11) and (25)) at the transition from DWT to SWT regimes (see section 3.5). A similar discontinuity is also found by *Ridolfi et al.* [2008] at the switch between atmospheric controlled exfiltration to groundwater depth controlled exfiltration, within a rigorous theoretical framework based on the Richard's equation.

5. Probability Distribution of the Water Table Depth

[45] With the modeling assumptions detailed in sections 3 and 4, the water balance equation (4) can be specified as follows: under shallow water table conditions ($y > y_c$) the balance equation is

$$n\left[1 - s_y(0)\right]\frac{\mathrm{d}y}{\mathrm{d}t} = \mathcal{P}(\lambda_0, \alpha) + k_l(y_0 - y - \psi_s) - T_p, \quad (31)$$

while under DWT conditions ($y < y_c$), the equation reads

$$\begin{aligned} n\left[1 - s_{fc} + B\left(\frac{\mathrm{d}h}{\mathrm{d}y} - 1\right)\right]\frac{\mathrm{d}y}{\mathrm{d}t} = \mathcal{P}\left(\lambda_0 \exp\left[\frac{nh\left(s_{fc} - \overline{s}'_m(h)\right)}{\alpha}\right], \alpha\right) + k_l \\ \cdot (y_0 - y - \psi_s) - T_p e^{h/b}. \end{aligned} \quad (32)$$

All terms appearing in equations (31) and (32) are either constant, or can be represented analytically as functions of y or h, with h being, in turn, a function of y through equation (26). Therefore equations (31) and (32) represent an univariate (in y), stepwise-continuous first-order stochastic differential equation, where the random forcing is a state-dependent multiplicative compound Poisson noise. The equation can be rewritten as

$$\frac{\mathrm{d}y}{\mathrm{d}t} = f(y) + g(y)\xi(y,t), \quad (33)$$

where

$$\begin{aligned} f(y) &= \begin{cases} \dfrac{k_l(y_0 - y - \psi_s) - T_p}{n\left[1 - s_y(0)\right]} & \text{if } y \geq y_c, \\ \dfrac{k_l(y_0 - y - \psi_s) - T_p e^{h/b}}{n\left[1 - s_{fc} + B\left(\dfrac{\mathrm{d}h}{\mathrm{d}y} - 1\right)\right]} & \text{if } y < y_c; \end{cases} \\ g(y) &= \begin{cases} \dfrac{1}{n\left[1 - s_y(0)\right]} & \text{if } y \geq y_c, \\ \dfrac{1}{n\left[1 - s_{fc} + B\left(\dfrac{\mathrm{d}h}{\mathrm{d}y} - 1\right)\right]} & \text{if } y < y_c; \end{cases} \\ \xi(y,t) &= \begin{cases} \mathcal{P}(\lambda_0, \alpha) & \text{if } y \geq y_c, \\ \mathcal{P}\left(\lambda_0 \exp\left[\dfrac{nh\left(s_{fc} - \overline{s}'_m(h)\right)}{\alpha}\right], \alpha\right) & \text{if } y < y_c. \end{cases} \end{aligned} \quad (34)$$

Equation (33) can be solved under steady state conditions to find out the probability density function (pdf) of the variable y. The solution for the case of a Poisson process with constant rate, λ, and zero mean is given by *Van Den Broeck* [1983].

[46] In the case of a generic state-dependent noise with rate $\lambda(y)$ (equation (23)), and a noise average $\alpha\lambda(y)$, the proba-

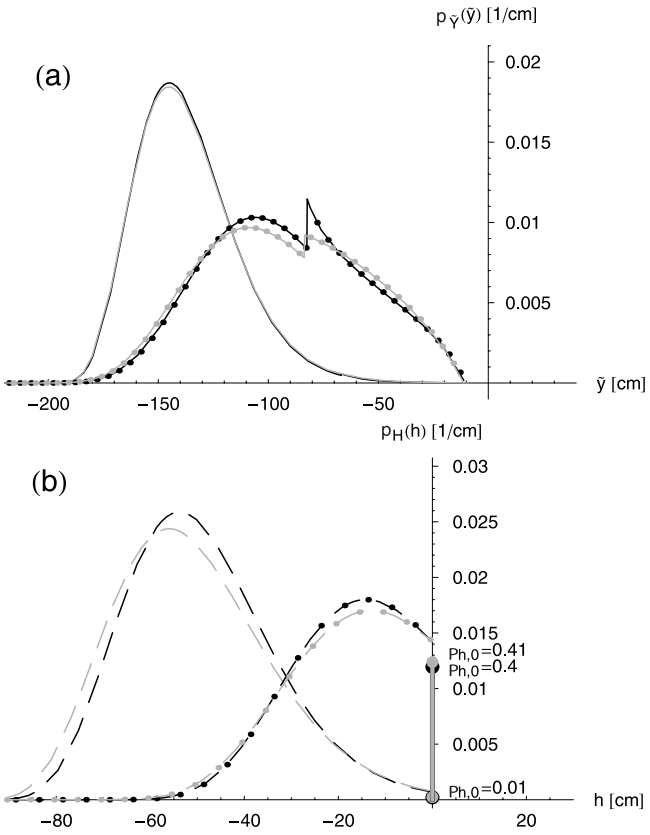

Figure 7. Probability density function of (a) the water table depth, $\tilde{y}$, and (b) the zero-flux surface, h, for a loamy sand (no markers) and a loam (with markers), according to *Rawls et al.* [1983] soil parameters. Other parameters are as follows: $\lambda_0 = 0.3\ d^{-1}$, $\alpha = 2$ cm, $T_p = 0.5$ cm/d, $b = 30$ cm, $y_0 = -200$ cm, $k_l = 3.7\ 10^{-3}\ d^{-1}$ (loamy sand) and $k_l = 7.9\ 10^{-4}\ d^{-1}$ (loam). Black lines are obtained by using equation (36), and gray lines are results from numerical solutions.

bility density function of y can be expressed as [*D'Odorico and Porporato*, 2004; *Porporato and D'Odorico*, 2004]

$$p_Y(y) = \frac{C}{f(y)} \exp\left[-\int_0^y \frac{f(u) + \alpha\lambda(u)g(u)}{\alpha g(u) f(u)} du\right], \qquad (35)$$

where C is a normalization constant obtained by setting $\int_{-\infty}^{0} p_Y(y)dy = 1$. According to the position of the water table given in equation (3) the probability distribution of the water table depth is obtained from $p_Y(y)$ as

$$p_{\tilde{Y}}(\tilde{y}) = p_Y(\tilde{y} - \psi_s), \qquad (36)$$

where the minimum water table depth is $\tilde{y} = \psi_s$, which corresponds to a complete saturation of the soil column. Ponding conditions are not allowed and the surface with null pressure head never reaches the soil surface.

[47] Once the pdf, $p_Y(y)$, has been determined, one can calculate the probability density function of h as a derived distribution of $p_Y(y)$ by using the relation

$$p_H(h) = p_Y[y(h)]\left(\frac{dh}{dy}\right)^{-1}. \qquad (37)$$

with $y(h)$ obtained by inverting equation (26). An atom of probability appears in the distribution of h at $h = 0$, with associated mass, $P_{h,0}$, corresponding to the probability of being in SWT conditions, i.e., $P_{h,0} = \int_{yc}^{0} p_Y(y)dy$.

[48] The probability distribution of the water table depth, and zero-flux surface position correspondingly, has a lower bound representing the deepest steady state water table position allowed by the system. This bound can be obtained by equating the lateral inflow to the root uptake from the saturated and HM zone. The properties of the steady state probability distributions of $\tilde{y}$ and h are investigated in the following sections.

5.1. Probability Distributions for Different Soil Conditions

[49] We first investigate the dependence of the water table depth on the soil type. Soil parameters affect all the components of the water balance, which, in turn, have a strong impact on the probability density function of water table depth, as shown in Figure 7a. In particular, the water table is closer to the soil surface in a loam than in a loamy sand. The analytical curves shown in Figure 7 (black lines) are obtained using equation (36), while the numerical solutions of the water balance equation (gray lines) are obtained (1) determining the numerical profile of soil moisture in the high moisture unsaturated zone using equations (17) and (25) under DWT conditions, and (2) numerically determining the corresponding specific yield (equation (15) under SWT conditions and equation (27) under DWT conditions), the $h(y)$ relation, and the value of the critical depth, y_c, without resorting to analytical approximations of the vertical profile of soil moisture, and without assuming a constant equivalent capillary flux, v^*. Figure 7 demonstrates that the analytical expressions provide a very good approximation of the probability distributions of y and h. The approximate analytical solution was also found to be robust with respect to a number of other conditions (see also Figures 9 and 10).

[50] The probability distribution of the position of zero-flux surface shown in Figure 7b, follows a similar pattern as the pdf of the water table depth, $\tilde{y}$ (Figure 7a). The reason for studying the probability distribution of h stems from the fact that h represents, in our modeling scheme, the upper limit of the groundwater influence on local soil water balances. For example, if the entire pdf of h is deeper than a certain z layer, one can assert that the source of root water uptake from that layer is not groundwater, but only rainfall. In addition, the zero-flux surface marks the transition between soil layers where the rate of root uptake matches the rate of potential transpiration (layers below h), and soil layers where some drought induced reduction of the transpiration rate occurs (layers above h). In the cases shown in Figure 7b, for example, the majority of the roots are in the first 30 cm of soil, thus in a loamy soil they are most of the time below h, while the opposite occurs in a loamy sand. As a consequence, the total root uptake will presumably be larger for the loam than for the loamy sand, since water stress reduces the uptake from the low moisture zone. More precise indications on root uptake and transpiration are provided in the companion paper [*Tamea et al.*, 2009].

[51] A more extensive analysis of the dependence of the water table dynamics on soil texture has been carried out by considering the mean and the coefficient of variation of $\tilde{y}$. To this end, soil hydraulic parameters were calculated using the pedotransfer functions provided by *Rawls and Brakensiek*

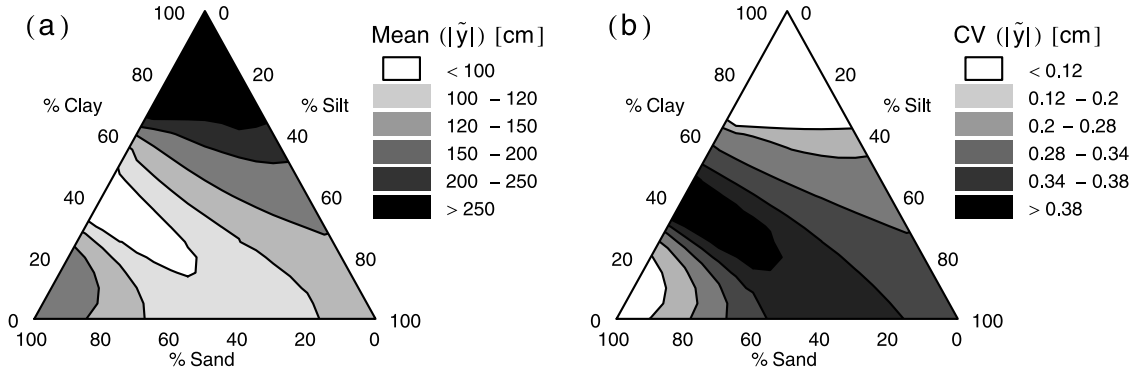

Figure 8. (a) Mean and (b) coefficient of variation of the probability density function of the water table depth, $\tilde{y}$, throughout the USDA soil texture triangle (soil parameters estimated with the pedotransfer function given by *Rawls and Brakensiek* [1989]). Other model parameters are as in Figure 7.

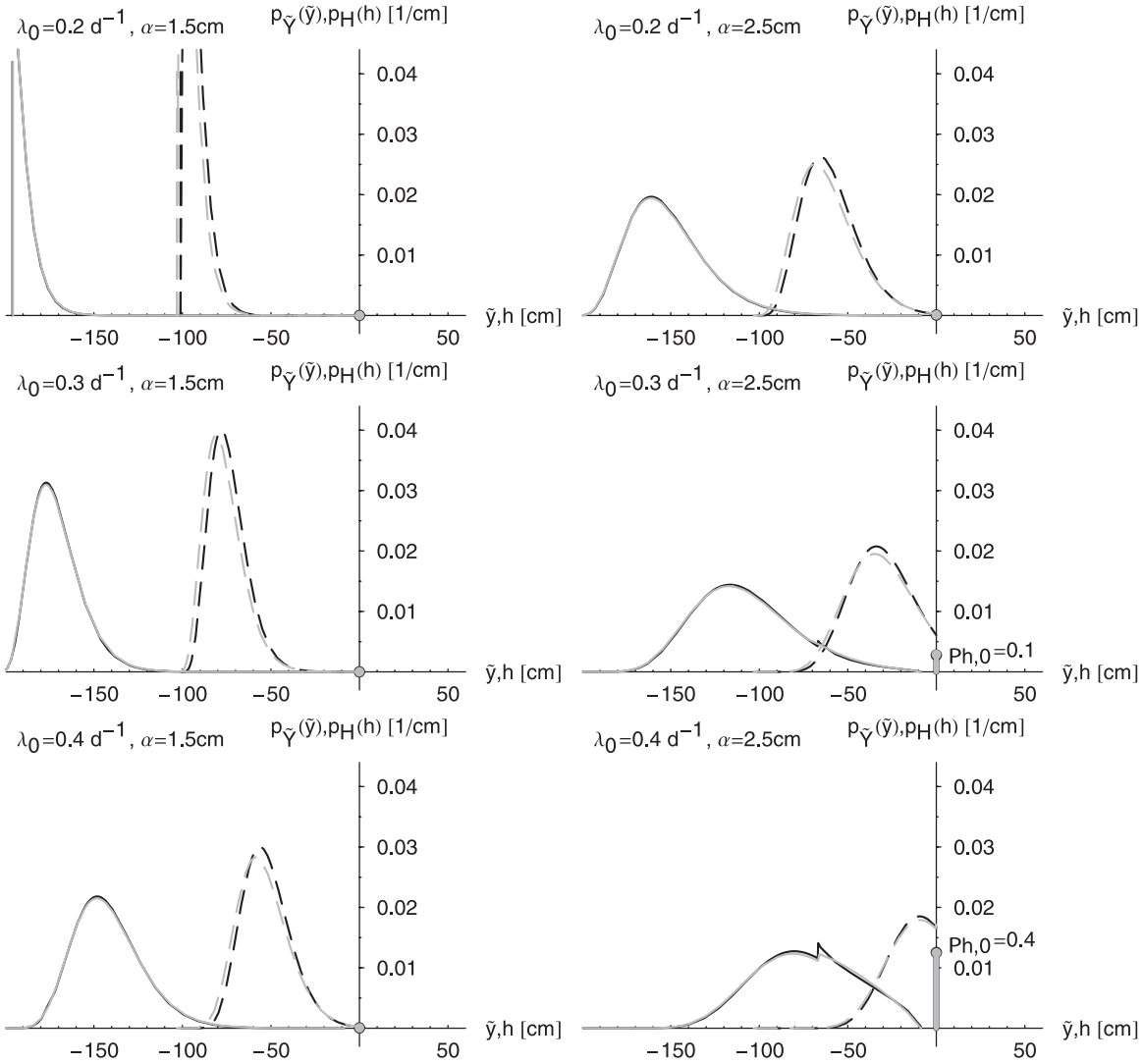

Figure 9. Probability density functions of the water table depth, $\tilde{y}$ (solid line), and the zero-flux surface, h (dashed line), for a loamy sand under different climatic conditions ($\lambda_0 = 0.2–0.3–0.4$ d^{-1}, $\alpha = 1.5–2.5$ cm). Other model parameters are as in Figure 7. The gray lines correspond to the exact numerical solution, while the black ones correspond to the analytical approximations.

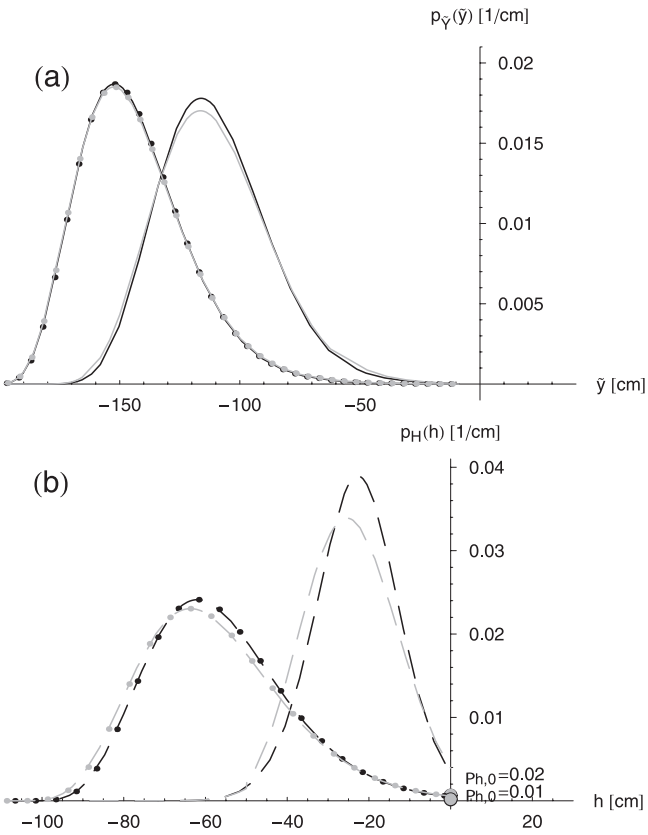

Figure 10. Probability density functions of (a) the water table depth, $\tilde{y}$, and (b) the zero-flux surface, h, for a shallow rooted vegetation (b = 10 cm, no markers) and a deep rooted vegetation (b = 40 cm, with markers). The soil is a loamy sand, and the other model parameters are as in Figure 7.

[1989], valid in the range shown in Figure 5a. The results are reported in Figure 8. The mean position of the water table is deeper in sandy and clayey soils. This effect is due to the high values of specific yield in sandy soils and to the low hydraulic conductivity of clays. The coefficient of variation, CV = Std($|\tilde{y}|$)/Mean($|\tilde{y}|$) (Figure 8b), is much smaller in sands due to smaller water table fluctuations in coarse-grained soil and higher volume of water required for a unit change in depth. Notice that the top part of the triangle has an uncertain reliability, due to the extrapolation of hydraulic parameter values, as discussed in the case of Figure 5.

5.2. Probability Distributions of $\tilde{y}$ and h Under Different Climate Conditions

[52] The stochastic fluctuations of the system are now examined under different climatic conditions. The analytical expressions of the steady state pdf of $\tilde{y}$ and h allow us to investigate how their dynamics are affected by a change in the rainfall parameters. In Figure 9, one can see that for very dry conditions the water table depth has little variability, with values comparable to the stage of the external water body (y_0). The zero-flux surface, at depth h, has also weak fluctuations under dry climatic conditions, and the large majority of plant roots remains in the low moisture zone for most of the time. Under these conditions, the stochastic models developed for the case of dryland ecosystems [e.g., *Rodriguez-Iturbe et al.*, 1999; *Laio*, 2006] can therefore be applied without substantial modifications. With increasing frequency of rainfall events, λ_0, (Figure 9, left), the pdfs of $\tilde{y}$ and h are shifted toward lower depths, but maintain a rather low dispersion around the central values. In contrast, when the average intensity of the rain events, α, increases (Figure 9, right) the variability of the water table position is strongly enhanced.

5.3. Impact of Plant Rooting Depth

[53] Understanding the impact of the mean rooting depth, b, on the pdf of the water table depth, is important in a number of ecohydrological applications, since it allows one to investigate how different plant functional types can affect the water table dynamics. Figure 10 shows the results of this analysis for two types of vegetation: herbaceous (b = 10, i.e., 95% of roots in the top 30 cm below the ground) and hardwood (b = 40, i.e., 95% of roots in the top 120 cm). Deep rooted vegetation takes up more water from the saturated zone, than shallow rooted plants. Thus, because deeper rooting systems are associated with higher fractions of transpiration contributed by the saturated zone, the resulting water table position is deeper.

6. Conclusions

[54] This paper develops a probabilistic framework for the evaluation of the dynamics of water table depth in humid land ecosystems. Similarly to earlier studies on the ecohydrology of arid and semiarid systems, a process-based model was developed for groundwater-dependent ecosystems, i.e., for ecosystems whose dynamics are strongly affected by the presence of a water table. Our model is based on the soil water balance of a homogeneous soil column. It accounts for the stochastic nature of rainfall, which is modeled as a state-dependent compound Poisson process. The water balance includes the effects of plant water uptake, capillary rise and lateral flow to or from an external water body. The water table dynamics are studied at a daily timescale allowing us to neglect intraday oscillations of water table depth and evapotranspiration, as well as subdaily patterns of rainfall and infiltration.

[55] A complete description of the soil water balance requires a model including the dynamics of two state variables: water table depth and soil moisture. Although these dynamics are intrinsically coupled, this paper concentrates on the probabilistic description of the water table depth, while the dynamics of the vertical profiles of soil moisture are investigated in the companion paper [*Tamea et al.*, 2009]. The coupling between the two variables occurs mainly through the infiltration process, which depends on the long-term average soil moisture profile in the low moisture zone.

[56] The steady state probability distribution of water table depth and the position of field capacity has been analytically derived and used to characterize the ecohydrology of groundwater-dependent ecosystems. Despite its dependence on a few simplifying assumptions, the probabilistic model developed in this paper provides a solid framework for the quantitative understanding of the complex dynamics underlying vegetation–water table interactions. In particular, this approach enables one to investigate the role of vegetation, climate and soil properties on the dynamics of groundwater-dependent ecosystems, and the

dependence of water table dynamics on different scenarios of climate change and water resources management. These results represent a first step toward the quantitative study of the ecohydrology of groundwater-dependent ecosystems with explicit consideration of its fundamental stochastic character.

[57] **Acknowledgments.** Francesco Laio acknowledges support from MIUR grant 2006089189. Stefania Tamea and Ignacio Rodriguez-Iturbe gratefully acknowledge the support of NSF (grant NSF-0642517). Paolo D'Odorico acknowledges support from the Virginia Coast Reserve LTER (NSF DEB-0621014).

References

Abramowitz, M., and I. A. Stegun (1965), *Handbook of Mathematical Functions*, Dover, New York.

Bierkens, M. F. P. (1998), Modeling water table fluctuations by means of a stochastic differential equation, *Water Resour. Res.*, *34*(10), 2485–2499.

Botter, G., A. Porporato, I. Rodriguez-Iturbe, and A. Rinaldo (2007), Basin-scale soil moisture dynamics and the probabilistic characterization of carrier hydrologic flows: Slow, leaching-prone components of the hydrologic response, *Water Resour. Res.*, *43*, W02417, doi:10.1029/2006WR005043.

Brooks, R. H., and A. T. Corey (1964), Hydraulic properties of porous media, *Hydrol. Pap. 3*, Colo. State Univ., Fort Collins.

D'Odorico, P., and A. Porporato (2004), Preferential states in soil moisture and climate dynamics, *Proc. Natl. Acad. Sci.*, *101*(24), 8848–8851.

Duke, H. R. (1972), Capillary properties of soil-influence upon specific yield, *Trans. ASAE*, 688–699.

Eagleson, P. S. (1978), Climate, soil and vegetation: 3. A simplified model of soil moisture movement in the liquid phase, *Water Resour. Res.*, *14*(5), 722–730.

Freeze, R., and J. Cherry (1979), *Groundwater*, Prentice-Hall, Old Tappan, N. J.

Guswa, A. J. (2005), Soil-moisture limits on plant uptake: An upscaled relationship for water-limited ecosystems, *Adv. Water Resour.*, *28*(6).

Guswa, A. J. (2008), The influence of climate on root depth: A carbon cost-benefit analysis, *Water Resour. Res.*, *44*, W02427, doi:10.1029/2007WR006384.

Hilberts, A. G. J., P. A. Troch, C. Paniconi, and J. Boll (2007), Low-dimensional modeling of hillslope subsurface flow: Relationship between rainfall, recharge, and unsaturated storage dynamics, *Water Resour. Res.*, *43*, W03445, doi:10.1029/2006WR004964.

Hillel, D. (1998), *Environmental Soil Physics*, Academic, San Diego, Calif.

Ho, M., B. Mc Cannon, and J. Lynch (2004), Optimization modeling of plant root architecture for water and phosphorus acquisition, *J. Theor. Biol.*, *226*(3), 331–340.

Kim, C. P., G. D. Salvucci, and D. Entekhabi (1999), Groundwater-surface water interaction and the climatic spatial patterns of hillslope hydrological response, *Hydrol. Earth Syst. Sci.*, *3*, 375–384.

Laio, F. (2006), A vertically extended stochastic model of soil moisture in the root zone, *Water Resour. Res.*, *42*, W02406, doi:10.1029/2005WR004502.

Laio, F., A. Porporato, L. Ridolfi, and I. Rodriguez-Iturbe (2001), Plants in water-controlled ecosystems: Active role in hydrologic processes and response to water stress ii. Probabilistic soil moisture dynamics, *Adv. Water Resour.*, *24*, 707–723.

Laio, F., P. D'Odorico, and L. Ridolfi (2006), An analytical model to relate the vertical root distribution to climate and soil properties, *Geophys. Res. Lett.*, *33*, L18401, doi:10.1029/2006GL027331.

Loheide, S. P., II, J. J. Butler Jr., and S. M. Gorelick (2005), Estimation of groundwater consumption by phreatophytes using diurnal water table fluctuations: A saturated-unsaturated flow assessment, *Water Resour. Res.*, *41*, W07030, doi:10.1029/2005WR003942.

Meinzer, O. E. (1927), Plants as indicators of ground water, *U.S. Geol. Surv. Water Supply Pap.*, *577*.

Mitsch, W. J., and J. G. Gosselink (2000), *Wetlands*, 3rd ed., John Wiley, Hoboken, N. J.

Nachabe, M. H. (2002), Analytical expressions for transient specific yield and shallow water table drainage, *Water Resour. Res.*, *38*(10), 1193, doi:10.1029/2001WR001071.

Naumburg, E., R. Mata-Gonzalez, R. G. Hunter, T. McLendon, and D. W. Martin (2005), Phreatophytic vegetation and groundwater fluctuations: A review of current research and application of ecosystem response modeling with an emphasis on great basin vegetation, *Environ. Manage.*, *35*(6), 726–740.

Porporato, A., and P. D'Odorico (2004), Phase transitions driven by state-dependent poisson noise, *Phys. Rev. Lett.*, *92*(11), 110,601, doi:10.1103/PhysRevLett.92.110601.

Porporato, A., F. Laio, L. Ridolfi, and I. Rodriguez-Iturbe (2001), Plants in water-controlled ecosystems: Active role in hydrologic processes and response to water stress iii. Vegetation water stress, *Adv. Water Resour.*, *24, 725–744.*

Rawls, W. J., and D. L. Brakensiek (1989), Estimation of soil water retention and hydraulic properties, in *Unsaturated Flow in Hydrologic Modeling*, edited by H. J. Morel-Seytoux, pp. 275–300, Kluwer Acad., Dordrecht, Netherlands.

Rawls, W. J., D. L. Brakensiek, and K. E. Saxton (1983), Estimation of soil water properties, *Trans. ASAE*, *25*(5), 1316–1320.

Ridolfi, L., F. Laio, and P. D'Odorico (2006), The effect of vegetation-water table feedbacks on the stability and resilience of riparian plant ecosystems, *Water Resour. Res.*, *42*, W01201, doi:10.1029/2005WR004444.

Ridolfi, L., P. D'Odorico, F. Laio, S. Tamea, and I. Rodriguez-Iturbe (2008), Coupled stochastic dynamics of water table and soil moisture in bare soil conditions, *Water Resour. Res.*, *44*, W01435, doi:10.1029/2007WR006707.

Robinson, T. W. (1958), Phreatophytes, *U.S. Geol. Surv. Water Supply Pap.*, *1423*.

Rodriguez-Iturbe, I., and A. Porporato (2004), *Ecohydrology of Water-Controlled Ecosystems: Soil Moisture and Plant Dynamics*, Cambridge Univ. Press, Cambridge.

Rodriguez-Iturbe, I., A. Porporato, L. Ridolfi, V. Isham, and D. R. Cox (1999), Probabilistic modelling of water balance at a point: The role of climate, soil and vegetation, *Proc. R. Soc. London, Ser. A*, *455*, 3789–3805.

Rodriguez-Iturbe, I., P. D'Odorico, F. Laio, L. Ridolfi, and S. Tamea (2007), Challenges in humidland ecohydrology: Interactions of water table and unsaturated zone with climate, soil, and vegetation, *Water Resour. Res.*, *43*, W09301, doi:10.1029/2007WR006073.

Salvucci, G. D., and D. Entekhabi (1994), Equivalent steady soil moisture profile and the time compression approximation in water balance modeling, *Water Resour. Res.*, *30*, 2737–2749.

Salvucci, G. D., and D. Entekhabi (1995), Hillslope and climatic controls on hydrologic fluxes, *Water Resour. Res.*, *31*(7), 1725–1739.

Schenk, H. J. (2005), Vertical vegetation structure below ground: Scaling from root to globe, *Prog. Bot.*, *66*, 341–373.

Schenk, H. J., and R. B. Jackson (2002), The global biogeography of roots, *Ecol. Monogr.*, *72*(3), 311–328.

Soil Conservation Service (1975), A basic system of soil classification for making and interpreting soil surveys, in *Agriculture Handbook*, vol. 436, pp. 466–742, U.S. Dep. of Agric., Washington, D. C.

Tamea, S., F. Laio, L. Ridolfi, P. D'Odorico, and I. Rodriguez-Iturbe (2009), Ecohydrology of groundwater-dependent ecosystems: 2. Stochastic soil moisture dynamics, *Water Resour. Res.*, *45*, W05420, doi:10.1029/2008WR007293.

Van Den Broeck, C. (1983), On the relation between white shot noise, Gaussian white noise, and the dichotomic Markov process, *J. Stat. Phys.*, *31*(3), 467–483.

Vartapetian, B. B., and M. B. Jackson (1997), Plant adaptation to anaerobic stress, *Ann. Bot.*, *79*(A), 3–20.

P. D'Odorico, Department of Environmental Sciences, University of Virginia, Charlottesville, VA 22904-4123, USA.

F. Laio, L. Ridolfi, and S. Tamea, Dipartimento di Idraulica, Trasporti ed Infrastrutture Civili, Politecnico di Torino, Corso Duca degli Abruzzi 24, I-10129 Torino, Italy. (francesco.laio@polito.it; stefania.tamea@polito.it)

I. Rodriguez-Iturbe, Department of Civil and Environmental Engineering, Princeton University, Princeton, NJ 08544, USA.